

## RHEOLOGICAL ANALYSIS OF XANTHATE TO OPTIMIZE VISCOSE HOMOGENIZATION

Jan PALÁTKA <sup>1</sup>, Karel MAYER <sup>1</sup>, Martin PEXA <sup>1</sup>, Eva OLMROVÁ <sup>1</sup>

<sup>1</sup> Department of Quality and Dependability of Machines, Faculty of Engineering, Czech University of Life Sciences, Kamýcká 129, 165 00, Prague, Czech Republic

### Abstract

The focus of the article is related to xanthation process used in viscose preparation. As part of this process, there is a sub-process referred to as the homogenization of alkaline cellulose, which is intended to produce homogeneous viscose. However, xanthate exhibits a significant number of particles and their clusters, whose main characteristic is toughness. Based on this, there is a need to consider the possibility of intensifying dispersion operations within individual devices of the viscose homogenization production line. Experimental results using a laboratory disperser showed that the apparent viscosity increased by approximately two orders of magnitude compared to the liquid phase. Specifically, at a shear rate of  $2 \text{ s}^{-1}$ , the apparent viscosity was measured to be approximately  $60 \text{ Pa}\cdot\text{s}$  and at  $4 \text{ s}^{-1}$ , it was  $40 \text{ Pa}\cdot\text{s}$ . The aim of this study is to determine rheological properties of xanthate, which will serve as a baseline for optimizing the intensification of the viscose homogenization process.

**Key words:** viscose; homogenizer; efficiency; intensification.

### INTRODUCTION

The xanthation process used to prepare viscose for spinning cord fiber involves treating alkaline cellulose with carbon disulfide, which generates an exothermic reaction that produces heat (Majumdar et al., 2022; Mendes et al., 2021; Wong et al., 2021). Until the viscose is ready for spinning, a process referred to as homogenization is repeated (Thielemans et al., 2022). Alkaline cellulose xanthation is accompanied by numerous side reactions (Shabbir & Mohammad, 2017; Wöss et al., 2016). They are responsible for the characteristic orange colour of xanthate and viscose produced from it (Krässig et al., 2004). The processing equipment may include hexagonal drums (with heated jackets, PTFE coating, and vacuum-tight construction). Dissolution is accelerated by stirring and trituration. To consider possibilities for intensifying dispersion operations within individual devices in the viscose homogenization production line, it is necessary to understand the dispersion mechanism. It is presumed that the reduction in the size of particles or clusters occurs due to the action of forces exerted by the active parts of technological devices and the surrounding liquid. The surface tension of the particles and their clusters, induced by the shear forces from the functional rotating parts of the rotor and stator, as well as by shear forces in the viscous liquid, must exceed their internal strength in order to achieve disintegration. The design of process parameters for dispersion equipment is based on this force balance (Paul et al., 2004). The aim of this study is to determine and verify the rheological properties of xanthate. This serves as a baseline for a further understanding necessary to determine the specific equipment to be selected for optimizing the intensification processes of viscose homogenization.

### MATERIALS AND METHODS

The homogenization process resulted in a homogeneous viscose, which, however, exhibited a significant amount of particles and their clusters. The clusters exhibited strongly elastic behaviour. Alkaline cellulose, together with additives, was dosed into the SiXa reactor R-101 (Fig. 1), where the batch was processed at an operating temperature range of  $21\text{--}38 \text{ }^{\circ}\text{C}$ , depending on the stage of the process. The duration of a batch was approximately 120–140 minutes. After the cold additives were added, the batch temperature dropped to around  $21 \text{ }^{\circ}\text{C}$ . The batch, at a given temperature, was pumped using a gear pump

P-103 through a spreader R-102 into a turbo dissolver device R-104, with the pumping time being approximately 20–26 minutes. In the turbo dissolver device, the batch was mixed with other additives and homogenized. Processing was carried out at a working temperature of 15–22 °C, depending on the stage of the process. Exothermic reactions occurred in the batch, and therefore, the batch was indirectly cooled by a cooling solution that flowed in the outer duplicator shell of the turbo dissolver device.

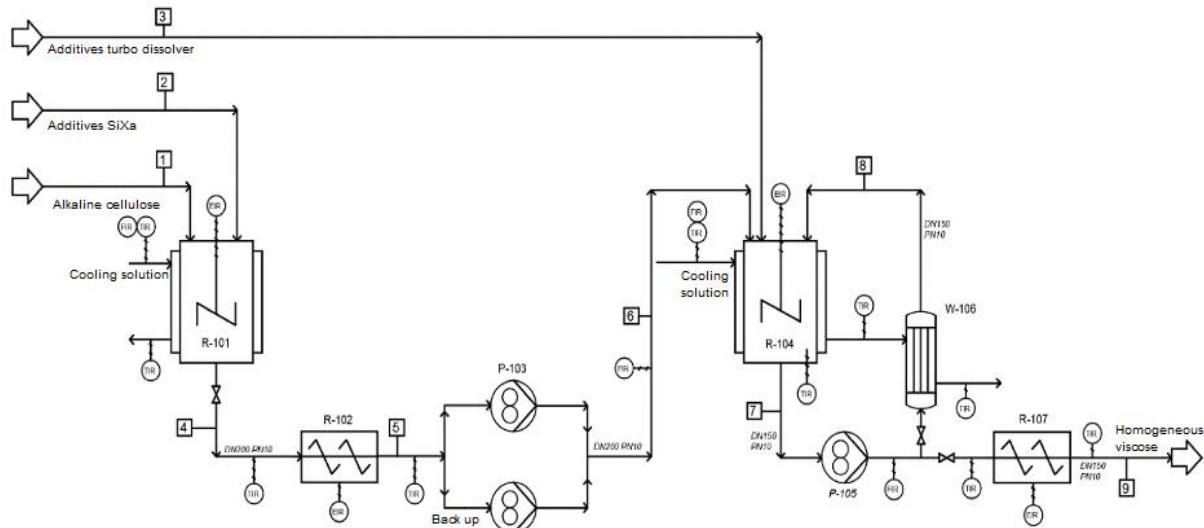


**Fig. 1** Process flow diagram (Jirout Tomáš & Krátký Lukáš, 2017).

The medium was cooled using an external heat exchanger W-106. The processing time of a batch in the turbo dissolver device was approximately 160 minutes. Once the required batch quality had been achieved, it was pumped through the R-107 homogenizer for further processing using the P-105 pump. A potential option was to shorten the time required for the primary preparation of the raw material in the SiXa reactor R-101. Partial dispersion occurred in the process gear pumps as well; however, most of the power input was dissipated in covering the energy associated with transporting the dispersion throughout the system, including overcoming mechanical energy losses, which were relatively high in the case of viscous substances. Only a small portion of the input power was used to generate shear effects that directly influenced particle dispersion. For this reason, particular attention needed to be paid to the intensification of dispersion in the spreader and turbo dissolver device, or alternatively, an additional dispersion device could be integrated into the external cooling circuit of the turbo dissolver. This was followed by an assessment of the effect of the Lenzing R-107 homogenizer when viscose was pumped from its preparation stage into tanks. Another consideration was the modification of its integration into the system and its potential use during the turbo dissolving process. From the dispersion samples taken after the SiXa reactor, the flow properties of the liquid phase were determined, and, in particular, the characteristics of the solid phase were observed. These particle clusters (*Fig. 2*) were found to be tough and to exhibit strongly elastic behaviour. Due to this, it was necessary to simultaneously generate shear and skid forces in a rotor and stator area of the device, as well as in the liquid phase, in order to disintegrate the clusters. To achieve effective disintegration of clusters in the viscose preparation process, the following mechanism was required in the dispersion device. In the primary spreader R-102, dispersion had to be carried out in several consecutive stages so that the coarsest fraction was broken down during the first stage, and the particle clusters were progressively reduced in size. Furthermore, during each dispersion stage, shear forces needed to be generated between the stator and rotor to first disrupt the surface integrity of the elastic particle clusters. Then, shear forces in the liquid gap between the rotor and stator further disintegrated—or broke up—the already disrupted clusters. The same principle,

though applied sufficiently within a single dispersion stage, could also be used in the R-104 turbo dis-solver device, as well as in its dispersion device located within the external cooling circuit.

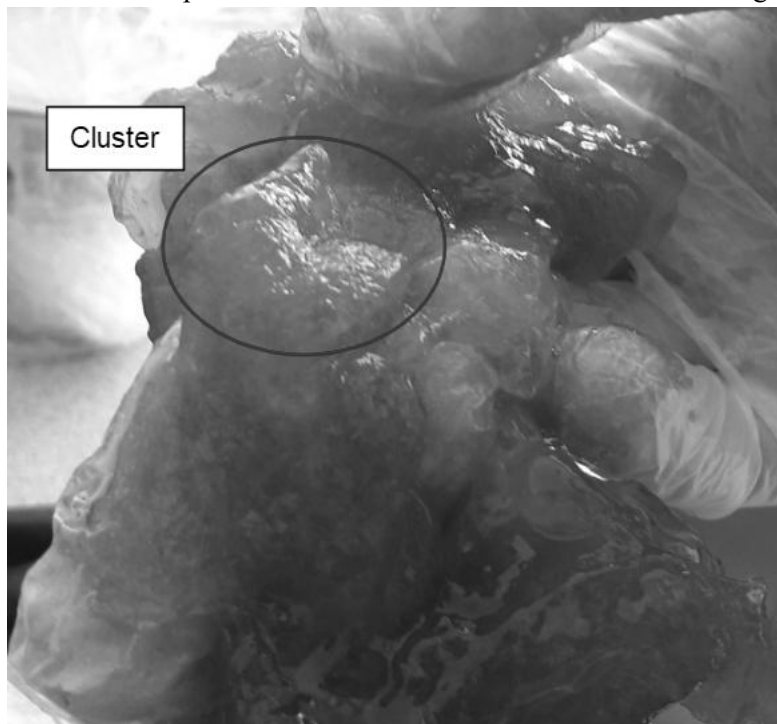


**Fig. 2** Cluster sample taken downstream of the SiXa reactor R-101.

In addition, due to the temperature load limit of the dispersion, the need for intensive cooling was taken into account when designing the optimization. For the dispersion experiments to verify a mechanism of cluster dispersion, an IKA S25N-25G laboratory dispersion device was used. In this dispersing adaptor, the shear effect at the blade edge of the rotor and stator grid, as well as the shear in the gap between the rotor and stator were combined. It was a laboratory device suitable for dispersing cellular and fibrous substances. The batch size ranged from 50 to 2000 ml. The stator diameter was 25 mm, the rotor diameter was 17 mm, and the gap size between the rotor and stator was 0.5 mm. The device was capable of reaching a maximum speed of 25,000 rpm, at which the rotor achieved a circumferential speed of  $22.2 \text{ m} \cdot \text{s}^{-1}$ . (*Description - S 25 N - 25 G Dispersing Tool, n.d.*) For viscosity determination, a Rheometer RC20 was used to perform the measurements. It was a rotational viscometer operating on the Searle principle and was used for rotational tests with controlled shear rate and controlled shear stress. This measuring device had an accuracy of  $\pm 1\%$  of the maximum value. (*RHEOMETER RC20 ENSURING QUALITY AND DEVELOPMENT, n.d.*)

## RESULTS AND DISCUSSION

The experimentally determined dependence of apparent viscosity  $\eta$  on shear rate  $\dot{\gamma}$  is shown in the graph (*Fig. 3*). From the experimental results, it is clear that the liquid phase of the dispersion exhibits pseudoplastic behaviour, as expected, which can be described by following power law model.

$$\eta = K \cdot \dot{\gamma}_1^{m-1} \quad (1)$$

Where:

$\eta$  - apparent viscosity [ $\text{Pa} \cdot \text{s}$ ],

$\dot{\gamma}$  - shear rate [ $\text{s}^{-1}$ ],

$K$  - consistency coefficient [ $\text{Pa} \cdot \text{s}^n$ ],

$m$  - flow index [-].

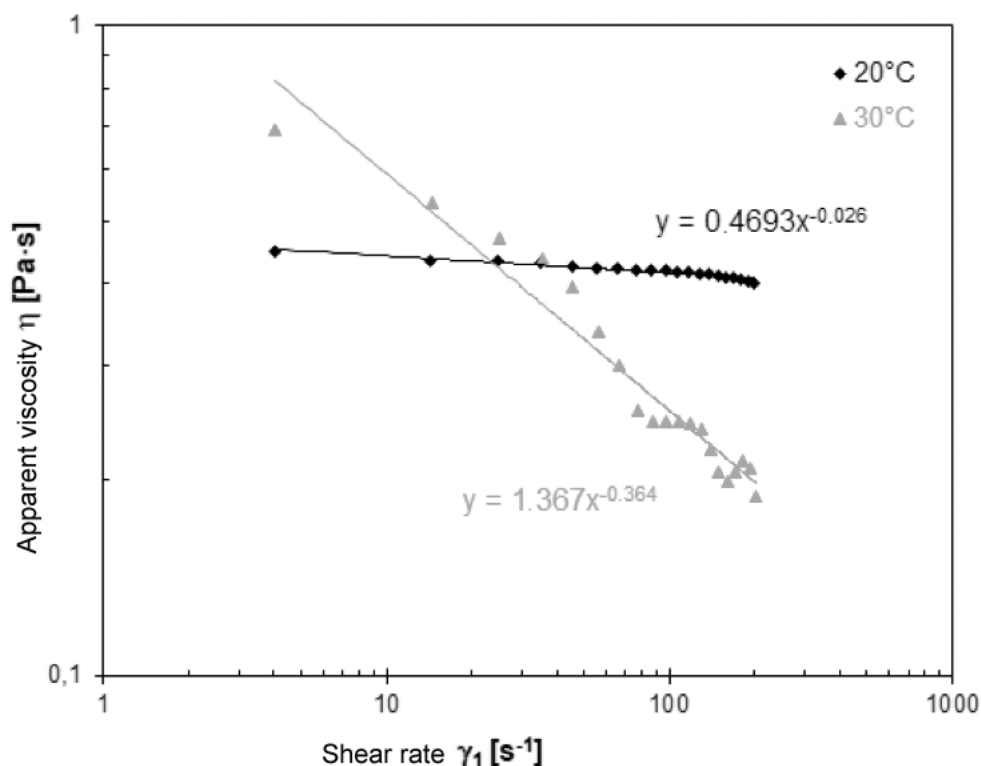


**Fig. 3** Dependence of the apparent viscosity of the liquid phase of the dispersion sample on shear rate and temperature.

The values of the model parameters can be found in the regression equations shown for the individual temperatures in the graph. However, during the rheological experiments, noticeable aging of the sample and changes in its flow properties over time were observed in a small volume. For this reason, the above results should be considered indicative, though sufficient reliable for the analysis and subsequent design of the dispersion device optimization concept. As already mentioned, in the dispersion adaptor used, the effect of shear on the edge of the rotor blade and the stator grid, as well as shear in the gap between the rotor and stator, were combined. This corresponds to the stated hypothesis of the dispersion mechanism. Figure 4 shows a photograph of the sample before and after dispersion, which was carried out in a laboratory environment at a rotor speed of 10,000 rpm. The dispersion process was performed over a period of 120 seconds. The dispersion time was limited by a maximum sample temperature increase of 10 °C, i.e. the dispersion was heated from 22.8 to 32.8 °C due to dissipated energy. The level of dispersion was assessed visually, and the apparent viscosity of the prepared dispersion was also determined using rotational rheometry. After dispersion, the apparent viscosity increased compared to the liquid phase; specifically, at a shear rate of 2 s<sup>-1</sup>, the apparent viscosity was measured to be approximately 60 Pa·s, and at 4 s<sup>-1</sup>, it was 40 Pa·s. Both assessments confirmed that a significantly higher level of dispersion was achieved. The dispersion experiments validated the stated hypothesis regarding dispersion mechanism and confirmed its applicability to the subsequent design of an intensified technology concept. Additionally, this laboratory procedure can be used to determine the process parameters required to achieve the desired force effects in the dispersion zone of the device. (*Jirout Tomáš & Krátký Lukáš, 2017*)

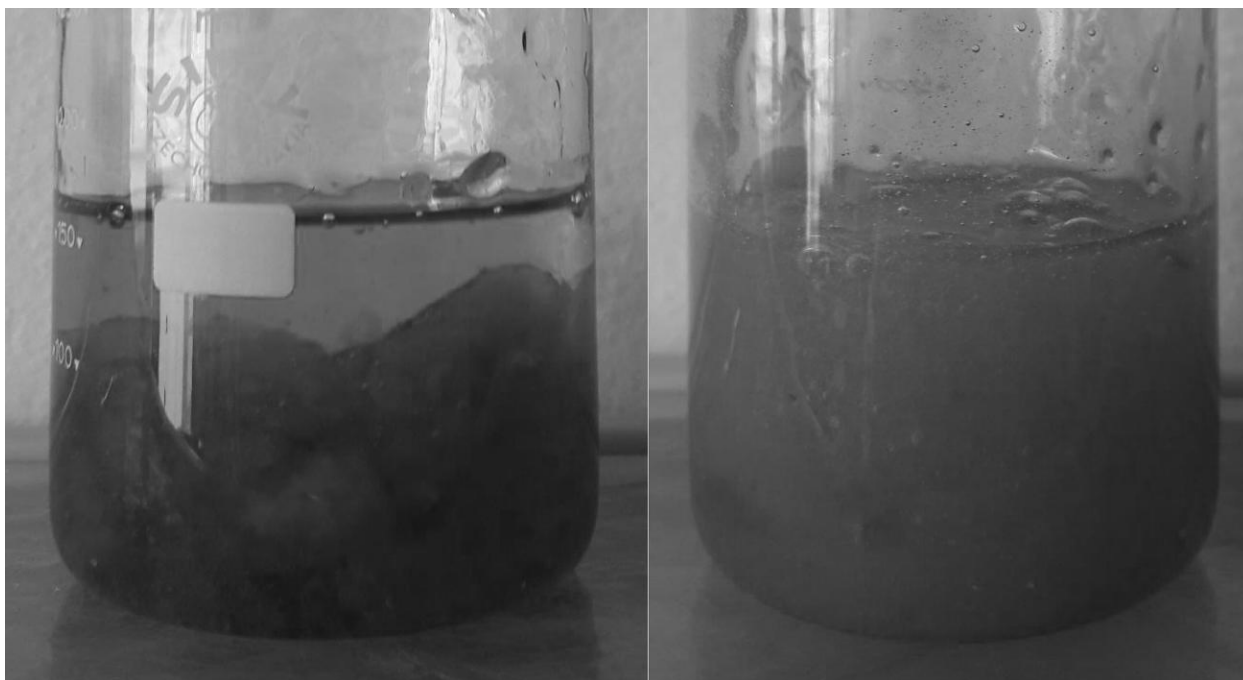


**Fig. 4** Photos from the dispersion experiment performed using the IKA S25N-25G laboratory dispersion device: left – before experiment, right – after experiment.

Compared with earlier studies from Krässig et al., 2004; Wöss et al., 2016; Thielemans et al., 2022; 2010 Rheo-optical study and Paul et al., 2004, the present results confirmed the pseudoplastic behavior of xanthate dispersions and observed higher apparent viscosities. The combined rotor–stator shear validated the cluster-disintegration mechanism, expanding established viscose-homogenization rheology insights

## CONCLUSIONS

The dispersion of xanthate was significantly enhanced by the combined shear effects at the rotor blade edge, stator grid, and within the rotor–stator gap, thereby confirming the proposed dispersion mechanism. Analysis of the prevailing viscose preparation technology indicated that process performance could be improved by reducing cycle time without increasing the volume of the SiXa reactor. Effective cluster disintegration required multi-stage dispersion process, in which the large particle aggregates were initially broken down, followed by successive stages of refinement. In each stage, shear forces needed to be precisely applied both at the rotor–stator interface and within the surrounding liquid medium to ensure complete disruption of elastic particle clusters. In light of these findings, future research should investigate the operational characteristics of the R-102 spreader and R-107 homogenizer, with particular emphasis on their impact on rotor–stator assembly optimization. A systematic study of these components could provide deeper insights into shear force distribution, energy efficiency and dispersion effectiveness, ultimately guiding improvements in viscose homogenization processing performance.

## ACKNOWLEDGMENT

Paper created on behalf of project „Optimization of processes and equipment in the viscose homogenization line” Glanzstoff – Bohemia s.r.o., Terežinská 60, 410 02 Lovosice, Czech Republic and grant from the IGA 2022 (*No. 2022:31190/1312/3109*) of the Czech University of Life Sciences Prague.



## REFERENCES

1. Description - S 25 N - 25 G Dispersing tool. (*n.d.*). Retrieved April 5, 2023, from <https://www.ika.com/en/Products-LabEq/Dispersers-pg177/S-25-N-25-G-Dispersing-tool-1713300/>
2. Jirout Tomáš, & Krátký Lukáš. (2017). OPTIMALIZACE PROCESŮ A ZAŘÍZENÍ V LINCĚ PŘÍPRAVY VISKÓZY.
3. Krässig, H., Schurz, J., Steadman, R. G., Schliefer, K., Albrecht, W., Mohring, M., & Schlosser, H. (2004). Cellulose. Ullmann's Encyclopedia of Industrial Chemistry. [https://doi.org/10.1002/14356007.A05\\_375.PUB2](https://doi.org/10.1002/14356007.A05_375.PUB2)
4. Majumdar, D., Bhanarkar, A., Rao, C., & Gouda, D. (2022). Carbon disulphide and hydrogen sulphide emissions from viscose fibre manufacturing industry: A case study in India. *Atmospheric Environment: X*, 13, 100157. <https://doi.org/10.1016/J.AEAOA.2022.100157>
5. Mendes, I. S. F., Prates, A., & Evtuguin, D. V. (2021). Production of rayon fibres from cellulosic pulps: State of the art and current developments. *Carbohydrate Polymers*, 273, 118466. <https://doi.org/10.1016/J.CARBPOL.2021.118466>
6. Paul, E. L., Atiemo-Obeng Victor A., & Kresta Suzanne M. (2004). *Handbook of Industrial Mixing: Science and Practice* | Wiley. A JOHN WILEY & SONS, INC., PUBLICATION.
7. RHEOMETER RC20 ENSURING QUALITY AND DEVELOPMENT. (*n.d.*). Retrieved April 9, 2025, from [www.rheotec.de](http://www.rheotec.de)
8. Shabbir, M., & Mohammad, F. (2017). Sustainable production of regenerated cellulosic fibres. *Sustainable Fibres and Textiles*, 171–189. <https://doi.org/10.1016/B978-0-08-102041-8.00007-X>
9. Thielemans, K., De Bondt, Y., Van den Bosch, S., Bautil, A., Roye, C., Deneyer, A., Courtin, C. M., & Sels, B. F. (2022). Decreasing the degree of polymerization of microcrystalline cellulose by mechanical impact and acid hydrolysis. *Carbohydrate Polymers*, 294, 119764. <https://doi.org/10.1016/J.CARBPOL.2022.119764>
10. Wong, L. C., Leh, C. P., & Goh, C. F. (2021). Designing cellulose hydrogels from non-woody biomass. *Carbohydrate Polymers*, 264, 118036. <https://doi.org/10.1016/J.CARBPOL.2021.118036>
11. Wöss, K., Weber, H., Grundnig, P., Röder, T., & Weber, H. K. (2016). Rapid determination of  $\gamma$ -value and xanthate group distribution on viscose by liquid-state <sup>1</sup>H NMR spectroscopy. *Carbohydrate Polymers*, 141, 184–189. <https://doi.org/10.1016/J.CARBPOL.2016.01.004>

## Corresponding author:

Ing. Jan Palátka, Department of Quality and Dependability of Machines, Faculty of Engineering, Czech University of Life Sciences Prague, Kamýcká 129, Praha 6, Prague, 165 00, Czech Republic, e-mail: [palatka@tf.czu.cz](mailto:palatka@tf.czu.cz)